Clinical Cancer Research

IL1 Receptor Antagonist Inhibits Pancreatic Cancer Growth by Abrogating NF-κB Activation

Zhuonan Zhuang[1,2], Huai-Qiang Ju[1,3], Mitzi Aguilar[1], Takashi Gocho[1,4], Hao Li[1,3], Tomonori Iida[1,4], Harold Lee[1], Xiaoqiang Fan[1], Haijun Zhou[1], Jianhua Ling[1], Zhongkui Li[1], Jie Fu[1], Min Wu[1], Min Li[5], Davide Melisi[6], Yoichiro Iwakura[7], Kesen Xu[8], Jason B. Fleming[9], and Paul J. Chiao[1,10]

Abstract

Purpose: Constitutive NF-κB activation is identified in about 70% of pancreatic ductal adenocarcinoma (PDAC) cases and is required for oncogenic KRAS-induced PDAC development in mouse models. We sought to determine whether targeting IL-1α pathway would inhibit NF-κB activity and thus suppress PDAC cell growth.

Experimental Design: We determined whether anakinra, a human IL-1 receptor (rhIL-1R) antagonist, inhibited NF-κB activation. Assays for cell proliferation, migration, and invasion were performed with rhIL-1R antagonist using the human PDAC cell lines AsPc1, Colo357, MiaPaCa-2, and HPNE/K-ras^{G12V}/p16sh. *In vivo* NF-κB activation–dependent tumorigenesis was assayed using an orthotopic nude mouse model ($n = 20$, 5 per group) treated with a combination of gemcitabine and rhIL-1RA.

Results: rhIL-1R antagonist treatment led to a significant decrease in NF-κB activity. PDAC cells treated with rhIL-1R antagonist plus gemcitabine reduced proliferation, migration, and invasion as compared with single gemcitabine treatment. In nude mice, rhIL-1R antagonist plus gemcitabine significantly reduced the tumor burden (gemcitabine plus rhIL-1RA vs. control, $P = 0.014$).

Conclusions: We found that anakinra, an FDA-approved drug that inhibits IL-1 receptor (IL-1R), when given with or without gemcitabine, can reduce tumor growth by inhibiting IL1α-induced NF-κB activity; this result suggests that it is a useful therapeutic approach for PDAC. *Clin Cancer Res; 22(6); 1432–44. ©2015 AACR.*

Introduction

Pancreatic ductal adenocarcinoma (PDAC) is the fourth leading cause of cancer death in the United States (1, 2). Mutational activation of KRAS is detected in almost 90% of PDAC cases (2). Recent studies have shown that mutant KRAS is required not only for the initiation of PDAC but also for maintaining the tumorigenic phenotype (3, 4). We previously identified the KRAS^{G12D}-induced constitutive NF-κB in PDAC cells and patient samples (5, 6). Our recent study demonstrated that NF-κB activation is required for mutant KRAS to induce PDAC (6).

As targeting mutant RAS proteins directly with small-molecule inhibitors has so far proved unsuccessful, one of the ideas is to identify key signaling pathways that function downstream of RAS and that inhibiting such signaling pathways may lead to tumor suppression (7, 8). NF-κB represents an important signaling pathway that is required by mutant KRAS in PDAC development (6). NF-κB transcription factors are involved in the regulation of cell proliferation, apoptosis, and inflammatory responses and in the stimulation of invasion and metastasis to promote multiple aspects of cancer development and progression (9). Some of the proinflammatory factors, such as IL-1 and TNFα, are regulated by NF-κB, also potent inducers of NF-κB, and strongly associated with most types of PDAC (10). For example, we showed that oncogenic KRAS activates NF-κB constitutively through the IL-1α autocrine mechanism *in vivo* (6), and overexpression of EGFR in PDAC induced IL-1α expression through AP-1 activity (10). Autocrine stimulation of IL-1α induced the constitutive activation of NF-κB (11). Furthermore, a number of chemotherapy agents, such as gemcitabine, a standard of care for PDAC (12), are able to activate NF-κB in pancreatic cancer cells and result in chemoresistance. Thus, NF-κB has been proposed as a target for PDAC.

NF-κB inhibition with nonspecific or specific inhibitors, such as glucocorticoids, natural products, is an attractive approach to cancer treatment (13). NEMO (IKKγ) or NF-κB essential modulator (NEMO) is a target that can be blocked by a cell-permeable

[1]Department of Molecular and Cellular Oncology, The University of Texas MD Anderson Cancer Center, Houston, Texas. [2]Department of General Surgery, Beijing Tsinghua Changgung Hospital Medical Center, Tsinghua University, Beijing, China. [3]Sun Yat-sen University Cancer Center, State Key Laboratory of Oncology in South China, Collaborative Innovation Center for Cancer Medicine, Guangzhou, China. [4]Department of Surgery, Jikei University School of Medicine, Tokyo, Japan. [5]Department of Surgery, The University of Oklahoma Health Sciences Center, Stanton L. Young Biomedical Research Center, Oklahoma City, Oklahoma. [6]Digestive Molecular Clinical Oncology Research Unit, Università degli studi di Verona, Verona, Italy. [7]Center for Experimental Medicine and Systems Biology, Institute of Medical Science, University of Tokyo, Minato-ku, Tokyo, Japan. [8]Department of Hepatobiliary Surgery, Qilu Hospital, Shandong University, Jinan, China. [9]Department of Surgical Oncology, The University of Texas MD Anderson Cancer Center, Houston, Texas. [10]Cancer Biology Program, the University of Texas Graduate School of Biomedical Sciences at Houston, Houston, Texas.

Note: Supplementary data for this article are available at Clinical Cancer Research Online (http://clincancerres.aacrjournals.org/).

Z. Zhuang and H. Ju contributed equally to this article.

Corresponding Author: Paul J. Chiao, The University of Texas MD Anderson Cancer Center, 1515 Holcombe Blvd., Houston, TX 77030. Phone: 713-794-1030; Fax: 713-794-4830; E-mail: pjchiao@mdanderson.org

doi: 10.1158/1078-0432.CCR-14-3382

Translational Relevance

KRAS mutation is found in almost 90% of pancreatic cancers. Modeling pancreatic cancer in mice with oncogenic KRAS recapitulated key features of the pathogenesis of this disease. Several recent studies have shown that NF-κB activation is required for oncogenic KRAS-driven pancreatic ductal adenocarcinoma (PDAC), as NF-κB inhibition led to tumor suppression. However, systematic inhibition of NF-κB will also affect function of normal cells, such as T cells, leading to complications when NF-κB inhibitors are used in treatment. Our results show that IL1α overexpression functions as a mechanistic link between constitutive activation of NF-κB and mutant KRAS in PDAC patients. IL-1α is targeted by an FDA-approved IL-1 receptor (IL-1R) antagonist as treatment for autoimmune disorders. On the basis of our findings and the existence of an IL-1R antagonist, pharmacologically targeting IL-1α overexpression by blocking IL-1R may improve PDAC patient survival.

NEMO-binding domain, inhibiting cell growth by downregulating NF-κB activation and NF-κB–dependent gene expression (14). Previous studies in our laboratory showed that inhibition of TAK1 kinase activity decreased the activation of the transcription factors NF-κB and AP-1 *in vivo* and may be a valid method of reducing the intrinsic chemoresistance of PDAC (15). Taken together, these studies suggest that NF-κB signaling pathway is a therapeutic target for inhibiting PDAC growth.

Systematic inhibition of NF-κB may cause severe side effects (9); thus, how to target NF-κB requires substantially more research before it is ready to be tested in clinical trials. One potential approach is to target IL-1 receptor (IL-1R), as it serves as a mechanistic link to mutant KRAS-induced NF-κB activation. Therefore, IL-1R antagonist, an FDA-approved drug for certain autoimmune diseases, may inhibit NF-κB activation by targeting the IL-1R (16) and may be useful clinically as a treatment for PDAC (17).

The aim of this study was to identify a novel therapeutic approach that targets key signaling pathways that function downstream of RAS and to determine whether inhibiting such signaling pathways may lead to tumor suppression of PDAC cells in orthotopic xenograft mouse model. We found that rhIL-1RA significantly reduced the tumorigenesis in PDAC cells and resistance of PDAC to chemotherapeutic agents both *in vitro* and *in vivo*.

Materials and Methods

Cell lines and reagents

The human PDAC cell lines AsPc1 and MiaPaCa-2 were purchased from the American Type Culture Collection. The Colo357 cell line was obtained from the laboratory of Dr. Isaiah J. Fidler. HPNE cell line was obtained from Dr. James W. Freeman at the University of Texas Health Science Center at San Antonio (Texas; ref. 18). Our lab built the HPNE/KRAS^{G12v}/P16sh cell line as previously reported (19). KRAS/P53$^{m/+}$ cell line was established from PDAC found in pancreas of Pdx1-cre/KRAS$^{LSL\text{-}G12D}$/p53$^{LSL\text{-}R273H}$ mice. Four low-passage PDX cells were obtained from Dr. Fleming's lab. All cell lines used in this study were maintained as monolayer cultures in DMEM (Caisson Labs, Inc.) that contained L-glutamine and 15 mmol/L HEPES and were supplemented with 10% heat-inactivated FBS and penicillin (100 IU/mL) and streptomycin (100 μg/mL) in an atmosphere of 5% carbon dioxide at 37°C. Anakinra, which was purchased from SOBI, is an rhIL-1R antagonist that is recommended for rheumatoid arthritis and cryopyrin-associated periodic syndromes. In general, 10 ng/mL of IL-1α is used to activate NF-κB. IL-1R antagonist is the most important regulatory molecule for IL-1α activity, and it is usually produced in a 10- to 100-fold molar excess (20). Because of the short half-life of IL1R antagonist, which is about 4 to 6 hours, we used 1,000-fold molar excess for complete inhibition *in vitro* experiments. A total of 1.5 mg/kg was used in orthotopic xenograft model of PDAC. This dosage is converted from human usage (100 mg/daily), and this conversion is based on the table in other research (21). Gemcitabine hydrochloride was purchased from SIGMA, Inc. N-acetyl-L-cysteine (NAC) was used to inhibit the ROS (Cell Signaling Technology). VivoGlo luciferin, *in vivo* grade (Promega, Inc.), is the potassium salt of D-luciferin, the firefly luciferase substrate that is capable of generating light when a suitable model is used. Isoflurane, liquid for inhalation, is manufactured by Baxter Healthcare Corporation.

Western blot analysis

The cell lysates from all human PDAC cell lines were lysed in radioimmunoprecipitation assay protein lysis buffer. The nuclear extracts were prepared according to the method of Andrews and Faller (22). Briefly, cells are pelleted for 10 seconds and resuspended in 400 μL cold Buffer A (10 mmol/L HEPES-KOH, pH 7.9, at 4°C, 1.5 mmol/L $MgCl_2$, 10 mmol/L KCl, 0.5 mmol/L dithiothreitol, 0.2 mmol/L PMSF) by mixing with a vorex. The cells are set on ice for 10 minutes for swelling and then vortexes for 10 seconds, are centrifuged for 10 seconds, and the supernatant fraction is saved as crude cytoplasm extract. The pellet is resuspended in 20 to 100 μL (according to starting number of cells) of cold Buffer C (10 mmol/L HEPES-KOH, pH 7.9, 25% glycerol, 420 mmol/L NaCl, 1.5 mmol/L $MgCl_2$, 0.2 mmol/L EDTA, 0.5 mmol/L dithiothreitol, 0.2 mmol/L PMSF) and incubated on ice for 20 minutes for high-salt extraction. Nuclear extracts are collected and cleared by centrifugation. The SDS-PAGE gel/Western blot analysis were performed according to the method of Burnette (23) and Towbin and colleagues (24). A total of 30 μg of protein extracts was loaded to each lane for electrophoresis then transferred to nylon membranes (Immobilon-P; Millipore) to detect NF-κB, the phosphorylation of, NF-κB, TAK-1 phosphorylation of, TAK1, cleaved caspase-3, PARP, cyclin D1, and Tab1 (Cell Signaling Technology), IL-1α, ERK phosphorylation, ERK, caspase-3, and IκBα (Santa Cruz Biotechnology).

PCR analysis

Total RNA was extracted from mouse tail tissue. RNA quality and quantity were measured using an ND-2000 spectrophotometer (Nanodrop). cDNA was synthesized using the PrimeScript RT Master Mix (Bio-Rad). cDNA (20 ng) was subjected to PCR with SYBR reagents and the IQ5 PCR system (Bio-Rad). The following primers were used: IL-1α MT primer, forward: 5′-CTTGGCCATACTGCAAAGGTCATG-3′ and reverse: 5′-GAGGTGCTGTTTCTGGTCTTCACC-3′; and IL1α wild-type (WT) primer, forward: 5′-ATTGTGAAAAGCCAGGGATG-3′ and reverse: 5′-CGTCAGGCAGAAGTTTGTCA-3′.

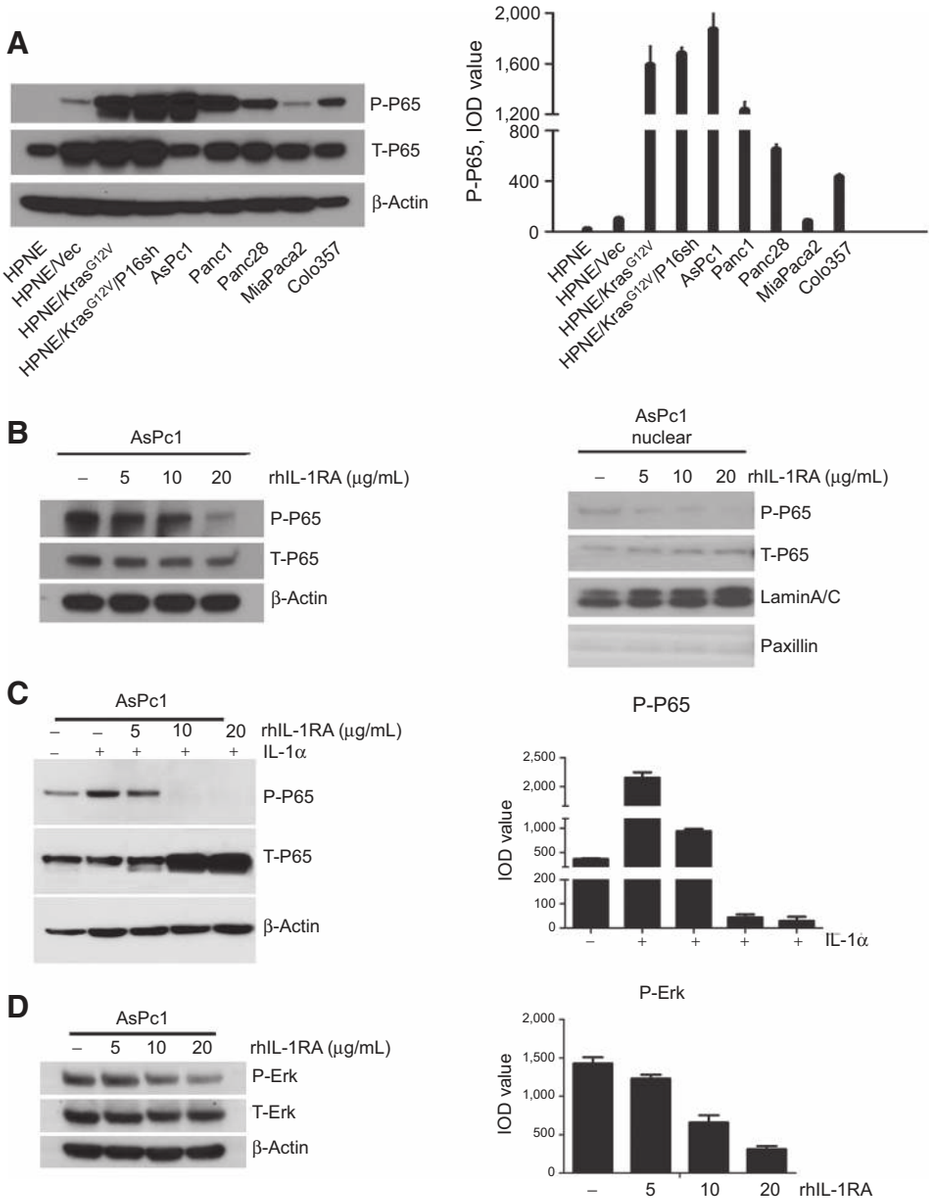

Figure 1.
Blocking the NF-κB–regulated IL-1α feed-forward loop with rhIL1RA decreased NF-κB and ERK pathway expression levels *in vitro*. A, Western blot analysis to determine the expression levels of phosphorylated P65 and P65 in different human PDAC proteins (right); the length of the bar indicates that there was high expression of phosphorylated P65 in human PDAC proteins (left). B, Western blot analysis to determine the expression of phosphorylated P65 and P65 in total cell lysates of the AsPc1 cell line, treated with rhIL1RA (left). Expressions of phosphorylated P65 and P65 in the nuclear extract in an AsPc1 cell line, as assayed by Western blot analysis (right). C, Western blot analysis showed the changes of P65 expression of AsPc1 cell line treated with IL-1α and rhIL-1R antagonist (left). P65 expression increased after stimulation with 10 ng/mL IL1 factor. After treatment for 4 hours, the expression of phosphorylated P65 decreased at doses of 10 and 20 μg/mL (right). D, Western blot analysis showed the changes of phosphorylated ERK expression of AsPc1 cell line treated with rhIL1R antagonist (left). The expression of phosphorylated ERK decreased with increasing doses of rhIL-1RA (right).

MTT assay for measuring proliferation. AsPc1 PDAC cells were seeded in 96-well plates (3×10^3 cells/well). After 12 hours, attached cells were treated with different concentrations of gemcitabine or rhIL-1R antagonist. Drug-treated cells were analyzed after being incubated for 24, 48, 72, or 96 hours. Next, a 5 mg/mL MTT solution was added to the cultures for an additional 3 to 4 hours. Finally, the medium containing MTT was aspirated off, and 100 μL of DMSO solution was added. Living cells formed crystals because of the presence of MTT. The absorbance of crystals dissolved by DMSO was read at 490 nm by an immunosorbent instrument.

Flow cytometry assay for measuring apoptosis. AsPc1 PDAC cells were incubated in 6-well dishes for 48 hours. Cells were washed twice with cold PBS and then resuspended in 1× binding buffer (0.1 mol/L Hepes, pH 7.4, 1.4 mol/L NaCl, 25 mmol/L $CaCl_2$) at a dose of 1×10^6 cells/mL. Next, 100 μL of the solution (1×10^5 cells) was transferred to a 5-mL culture tube, and 5 μL propidium iodide (BD Pharmingen, Inc.) and 5 μL APC Annexin V (BD Pharmingen, Inc.) were added. The cells were gently vortexed and incubated for 15 minutes at 25°C in the dark. After the tubes had been incubated, 400 μL of 1× binding buffer was added; the tubes were analyzed by flow cytometry within 1 hour.

Colony-formation assay. Using 6-well dishes, AsPc1 PDAC cells were cultured at 500 cells per well. They were then treated with 5 μg, 10 μg, or 20 μg/mL rhIL1RA, with or without 10 μmol/L of gemcitabine, for 2 weeks. A statistical analysis was performed by counting the number of colonies that were fixed with formalin (Sigma) within 30 minutes and stained with crystal violet (Sigma) within 1 hour.

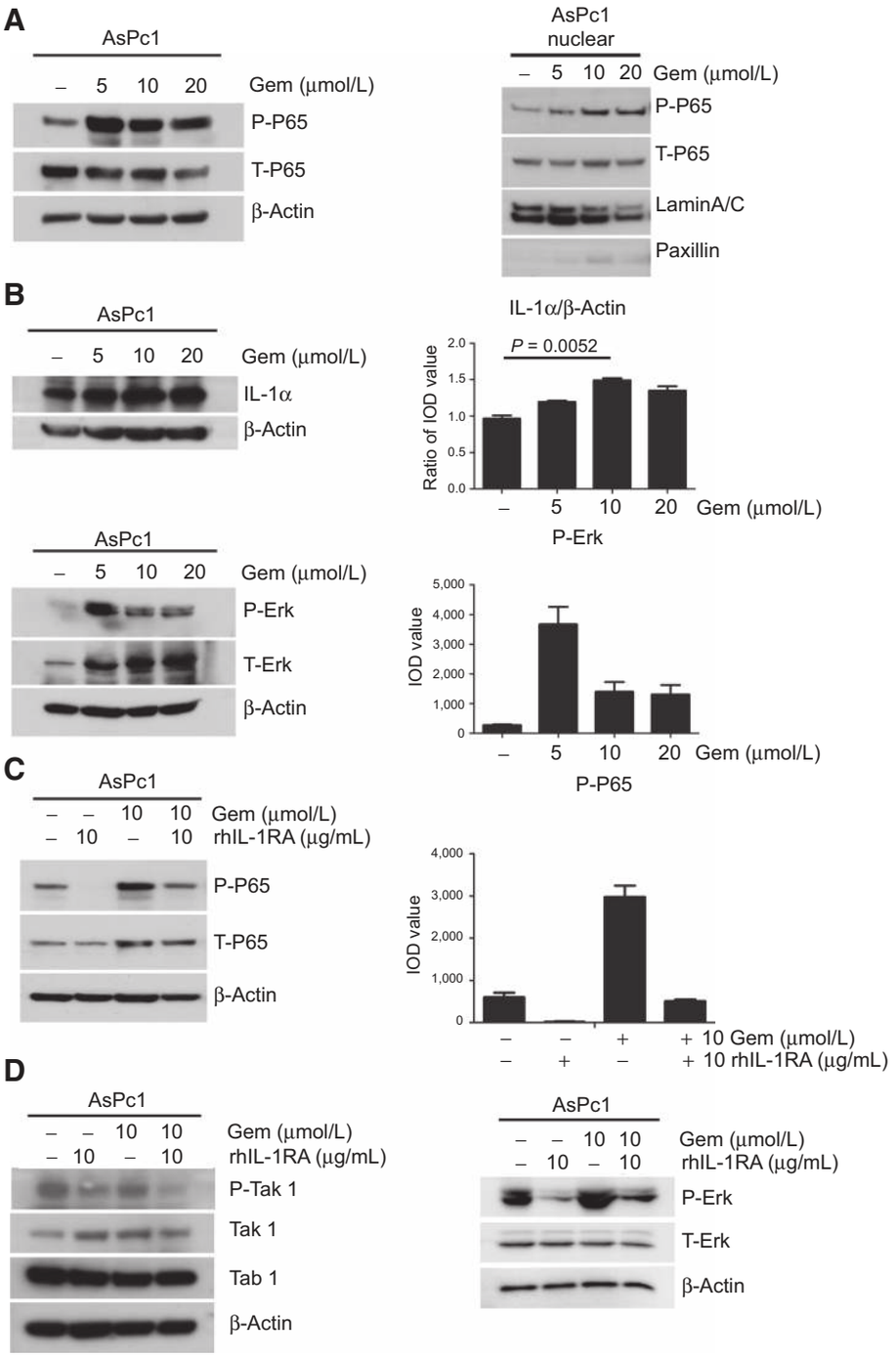

Figure 2.
NF-κB and ERK pathway changes *in vitro* after treatment with gemcitabine. A, Western blot analysis to determine the expression of phosphorylated P65 and P65 in total cell lysates of AsPc1 cells after treatment with gemcitabine (left); Western blot analysis to determine the expression of phosphorylated P65 and P65 in nuclear extracts in the AsPc1 cell line (right). B, Western blot analysis showed the changes of IL-1α expression in AsPc1 treated with gemcitabine (top left). The bar table showed IL-1α expression increased after the activated NF-κB was treated with gemcitabine (top right); Western blot analysis showed phosphorylated ERK and ERK expressions in AsPc1 cells treated with gemcitabine (bottom left). The bar table showed gemcitabine increased phosphorylated ERK and ERK expressions in AsPc1 cells (bottom right). C, Western blot analysis showed the changes of expression of NF-κB in AsPc1 cells (left). The bar table showed rhIL-1R antagonist decreased the expression of NF-κB in AsPc1 cells treated with gemcitabine combined with rhIL-1R antagonist (right). D, NF-κB pathway and the cell-cycle effect, as assayed by Western blot analysis in ASPC1 cells treated with gemcitabine and rhIL-1RA (left); expression of ERK, as assayed by Western blot analysis, in AsPc1 cells treated with gemcitabine combined with rhIL-1RA (right).

Matrigel invasion test. AsPc1 PDAC cells in 24-well dishes (1×10^5 cells/well) were treated with 10 μmol/L of gemcitabine, with or without 5, 10, or 20 μg/mL of rhIL1R antagonist overnight. The invasion capability was observed on a Biocoat Matrigel (a soluble basement membrane) invasion chamber (Fisher Scientific).

Wound-healing assay. AsPc1 PDAC cells were cultured on 6-well plates (3×10^5 cells/well) until the cells were confluent. The monolayers were scratched horizontally with a 1-mL pipette tip. The media were replaced after the dislodged cells were aspirated and cleaned. The AsPc1 cells were then incubated with 10 μmol/L of gemcitabine, with or without 5 μg, 10 μg, or 20 μg/mL rhIL-1R antagonists. The cells were incubated overnight; cell invasion was observed and images were photographed in each well using a phase contrast–inverted microscope.

TUNEL assay. Slices of AsPc1 PDAC tissue were stained by the terminal deoxynucleotidyl transferase–mediated dUTP nick end

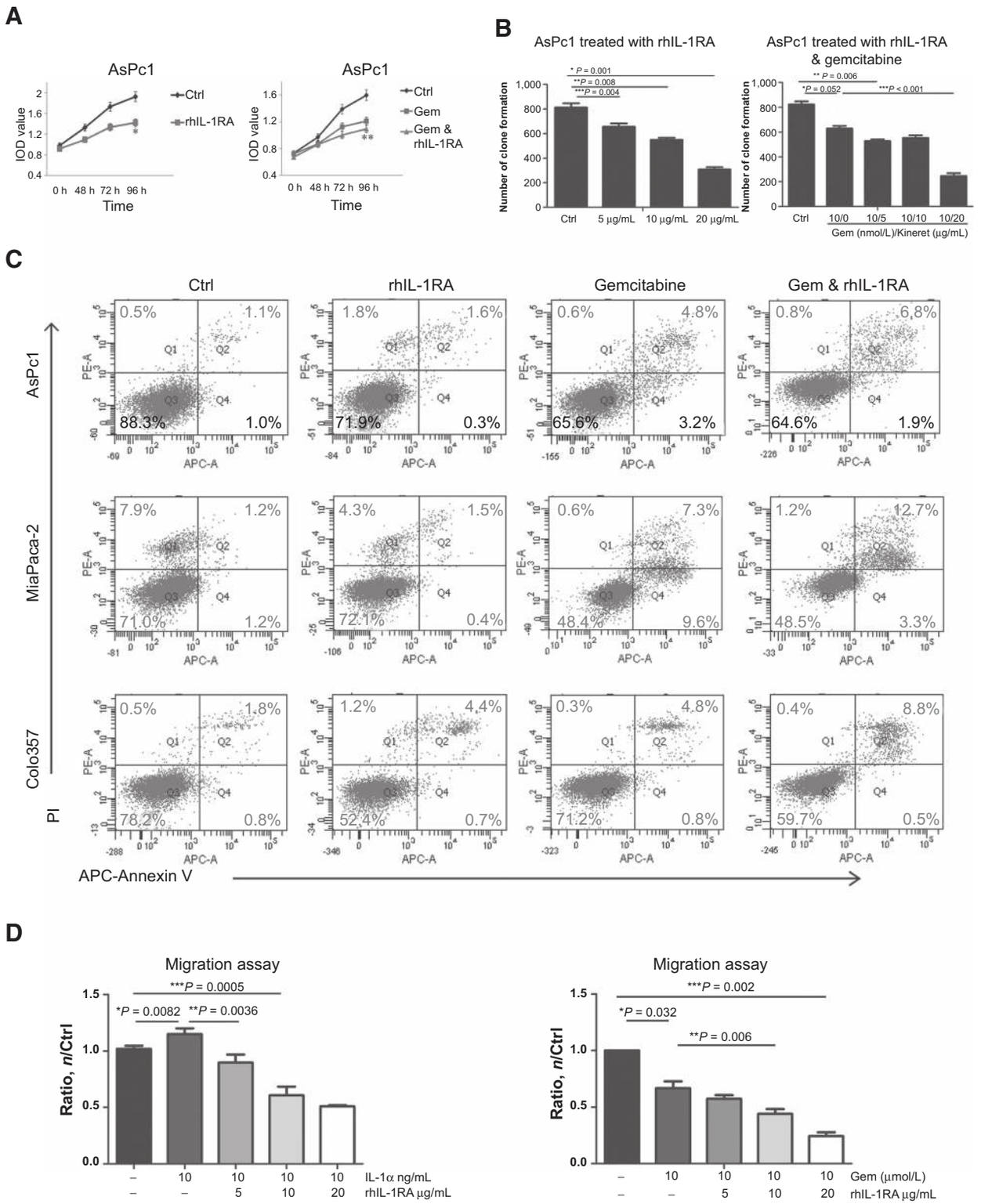

Figure 3.

Apoptosis of AsPc1 cells after blocking the NF-κB–regulated IL-1α feed-forward loop and treatment with gemcitabine *in vitro*. A, cell growth was assessed by the MTT assay. The growth of AsPc1 cells treated with rhIL-1RA daily was significant slowly compared with control group (left, *, $P = 0.002$); gemcitabine combined with rhIL-1RA decreased AsPc1 cell proliferation significantly (right). (*Continued on the following page.*)

labeling (TUNEL) assay using the Situ cell death detection Kit and fluorescein (Roche Diagnostics) to evaluate apoptosis induction. The number of TUNEL-positive cells was counted and photographed.

Histologic and immunohistochemical analyses. The PDAC tissues were excised 1 day after the end of treatment. Formalin-fixed, paraffin-embedded tissue sections were subjected to immunostaining using the streptavidin–peroxidase technique, with diaminobenzidine as a chromogen. Hematoxylin and eosin (H&E) and immunohistochemical analyses were conducted according to standard procedures. For antigen retrieval, the sections were subjected to heat in 0.01 mol/L citrated buffer. Sections were incubated at 4°C overnight with the primary rabbit anti-human monoclonal antibody anti–NF-κB phos-p65 (Cell Signaling Technology; 1:100 dilution), the primary mouse anti-human monoclonal antibody anti–p-ERK (Santa Cruz Technology; 1:150 dilution), or the primary mouse anti-human monoclonal antibody anti-Ki67 (NeoM; 1:200 dilution). Slides were washed in Tris-buffered saline buffer and incubated for 30 minutes with the appropriate horseradish peroxidase–conjugated secondary antibody before being counterstained with Meyer's hematoxylin (Peroxidase Detection System; Leica Microsystems, Inc.). To ensure antibody specificity, consecutive sections were incubated with isotype-matched control immunoglobulins and no primary antibody. The expression levels of Ki67, activated p65, and ERK were detected as nuclear brown staining of varying intensities in neoplastic cells. The slides were evaluated independently using light microscopy.

PDAC orthotopic xenograft model. Twenty 4- to 6-week-old male athymic nude mice (NCI-nu), which weighed approximately 24.9 to 33.0 g, were purchased from the Animal Production Area of the National Cancer Institute-Frederick Cancer Research Facility (Frederick, MD). Five 4- to 6-week-old male WT mice were purchased from The Jackson Laboratory, Inc. An additional 5 male IL-1$\alpha^{-/-}$ mice were purchased from the Laboratory Animal Research Center, Institute of Medical Science, University of Tokyo (Tokyo, Japan).

All mice were housed and treated in accordance with the guidelines of The University of Texas MD Anderson Cancer Center's Animal Care and Use Committee and were maintained in specific pathogen-free conditions. The facilities were approved by the Association for Assessment and Accreditation of Laboratory Animal Care; they meet all current regulations and standards of the US Departments of Agriculture and Health and Human Services and the NIH.

For the nude mouse orthotopic xenograft model, AsPc1 PDAC cells were harvested in PBS with 20% Matrigel (Fisher Scientific). Tumor cells (1.0×10^6 cells in 50 μL of PBS) were then injected subcapsularly into the pancreatic tissue of nude mice, under the spleen. We used 1-mL syringes and 30-gauge needles (Hamilton Company) to inject AsPc1 PDAC cells. Wound clips (Braintree Scientific, Inc.) were used to close the abdominal incisions and were removed after the incisions had healed, about 10 days later. For the *in vivo* studies, 1.5 mg/kg i.p. rhIL-1R antagonist and 25 mg/kg i.p. gemcitabine, diluted with PBS, were used to treat the nude mice daily for 4 weeks. All mice were weighed weekly and observed for tumor growth during the 4-week treatment. A cryogenically cooled IVIS 100 imaging system was used to detect the orthotopic xenograft tumor size as emitted photons collected and sent through a camera to a data acquisition computer running Living Image Software (Xenogen).

For the genetically engineered mouse orthotopic xenograft model, KRAS/p53$^{m/+}$ mouse tumor cells were harvested in PBS with 20% Matrigel. The injection method was the same as that for the nude mouse orthotopic xenograft model. After 3 weeks, all mice were euthanized by carbon dioxide inhalation, and the tumor tissues were dissected.

Statistical analysis. All statistical analyses were conducted using SPSS 19.0 software. The significance of the data was determined using a paired or independent sample *t* test. For error bars in all experiments, values represent the mean ±SD, as determined by GraphPad Prism 5 software (GraphPad Software). All statistical tests were two-sided, and $P < 0.05$ was considered statistically significant.

Results

Inhibition of IL-1R activation downregulates NF-κB and IL-1α autocrine stimulation of PDAC cells

In a panel of nine human PDAC cell lines and two immortalized human pancreatic epithelial cell lines (HPNE and HPNE/Vec), we observed high levels of phosphorylated p65NF-κB, indicating that NF-κB is activated in these PDAC cell lines (Fig. 1A). This is consistent with the electrophoretic mobility shift assay results from our previous study (6, 25). Our recent study showed that the NF-κB–regulated IL1α feed-forward loop was essential for inducing and sustaining constitutive NF-κB activation in PDAC cells expressing mutant KRAS (6). To verify whether inhibition of the IL-1α autocrine stimulation suppressed NF-κB activation, we treated AsPc1 cells with rhIL-1R antagonist. NF-κB activity was reduced in cells treated with rhIL-1RA at doses of 5, 10, and 20 μg/mL for 4 hours (Fig. 1B, left) and in the nuclear extract of AsPc1 cells (Fig. 1B, right). Even when stimulated by IL-1α (10 ng/mL), NF-κB activation in AsPc1 cells was suppressed by rhIL-1RA at doses of 10 and 20 μg/mL (Fig. 1C). We also treated 4 PDX cell lines with rhIL-1RA at doses of 5, 10, and 20 μg/mL, and the phosphorylated NF-κB was inhibited by rhIL1RA (Supplementary Fig. S1). In addition, we found that activation of phosphorylated ERK was inhibited by rhIL-1RA at 4 hours (Fig. 1D). Taken

(*Continued.*) Gemcitabine and rhIL-1RA vs. control, **, $P = 0.013$. B, cell proliferation was assessed by the colony-formation test. Error bar, cell colony formation slowed in AsPc1 cells after treatment with rhIL1RA daily compared with in the control ($P = 0.001$, left). Gemcitabine and rhIL-1RA influenced colony formation more significantly than did gemcitabine alone ($P < 0.001$, right). C, flow cytometry analysis of the Annexin V staining assay. The ratio of Q2+Q4 in the AsPc1 cell line (Ctrl: 2.1%; rhIL-1RA: 1.9%; gemcitabine: 8%; gem+rhIL-1RA: 8.7%); the ratio of Q2+Q4 in the MiaPaca2 cell line (Ctrl: 2.4%; rhIL-1RA: 1.9%; gemcitabine: 14.2%; Gem+rhIL-1RA: 16%); and the ratio of Q2+Q4 in the Colo357 cell line (Ctrl: 2.6%; rhIL-1RA: 5.1%; gemcitabine: 5.6%; Gem+rhIL-1RA: 9.3%). rhIL-1RA can be combined with gemcitabine to increase PDAC cell apoptosis. D, assay of the Matrigel invasion chamber test showed reduced migration and invasion of AsPc1 cells treated with IL1α and rhIL-1RA (top). Assay of the Matrigel invasion chamber test showed reduced migration and invasion of AsPc1 cells treated with gemcitabine and rhIL-1RA (lower).

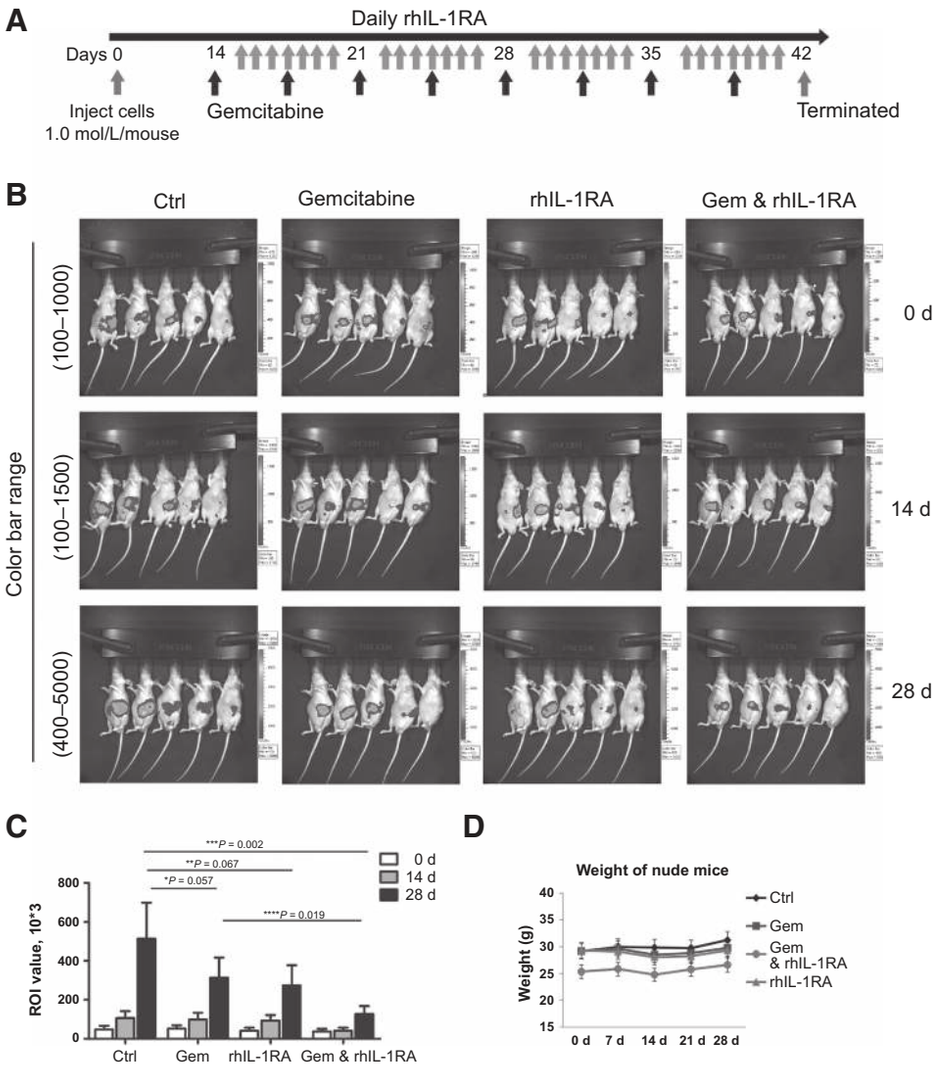

Figure 4.
Inactivation of the NF-κB-regulated IL-1α feed-forward loop and treatment with gemcitabine decreased tumorigenesis in AsPc1 cells in the orthotopic mouse model. A, tumor progression timeline with experimental treatment time points. Nude mice were treated with 25 mg/kg gemcitabine twice per week and/or with 1.5 mg/kg rhIL-1RA daily in total 4-week treatment. B, a digital gray-scale image of each mouse was acquired, which was followed by the acquisition and overlay of a pseudocolor image that represented the spatial distribution of detected photons emerging from active luciferase in the nude mice at 1, 14, and 28 days after treatment. C, error bar shows that the bioluminescence imaging value of *in vivo* tumor growth was significantly lower in mice treated with gemcitabine and rhIL-1RA than in the control and gemcitabine groups ($P = 0.002$; $P = 0.019$). D, there was no significant weight loss in 20 athymic mice.

together, these results demonstrate that inhibition of IL1R activity is able to decrease NF-κB activity and IL-1α expression of PDAC cells, suggesting that IL-1R is a potential surrogate therapeutic target for NF-κB.

Gemcitabine induced NF-κB and ERK activity in PDAC cells

To demonstrate whether gemcitabine-activated NF-κB can be inhibited by rhIL-1RA, we initially treated the AsPc1 cell line with three different doses of gemcitabine (5, 10, and 20 μmol/L) for 4 hours. We found an increase in phosphorylated NF-κB levels in the whole-cell and nuclear extracts of gemcitabine-treated AsPc1 cells (Fig. 2A), which is consistent with the previous study that shows gemcitabine induces NF-κB activation (26). To confirm the involvement of ROS in the activation of NF-κB, we detected NF-κB activation status and found suppression in AsPc1 cells incubated with NAC 1 hour prior to gemcitabine treatment (Supplementary Fig. S2A). In Colo357 and MiaPaCa-2 cells treated with gemcitabine, NF-κB phosphorylation was also increased (Supplementary Fig. S2B and S2C). Importantly, IL1α was overexpressed in a number of these human PDAC cells, such as AsPc1 cells treated with gemcitabine, congruous with the NF-κB–regulated IL-1α feed-forward loop (Fig. 2B, top; ref. 6). We also observed an increase of ERK phosphorylation, which is inducible by IL-1 in AsPc1 cells treated with gemcitabine for 4 hours (Fig. 2B, bottom). To determine whether rhIL-1RA can inhibit NF-κB activation to modulate gemcitabine chemoresistance, we treated AsPc1 PDAC cells with 10 μg/mL rhIL-1R antagonist in combination with 10 μmol/L of gemcitabine. We found constitutive NF-κB activity inhibited by rhIL-1RA, and the gemcitabine-induced NF-κB activation was substantially reduced in gemcitabine- and rhIL-1R antagonist–treated group (Fig. 2C). To determine whether a key IL-1R signaling node, such as TAK1, is involved in gemcitabine-induced NF-κB activation, we examined activation status of TAK1 and ERK. The results showed that the activated or phosphorylated TAK1 was substantially reduced by rhIL1R antagonist, and the gemcitabine-induced TAK1 activation was inhibited in rhIL-1R antagonist–treated AsPc1 cells (Fig. 2D). The expression of Tab1 did not significantly change with and without gemcitabine and rhIL-1RA (Fig. 2D, left). Furthermore, our results show that ERK activation was inhibited by rhIL-1R antagonist,

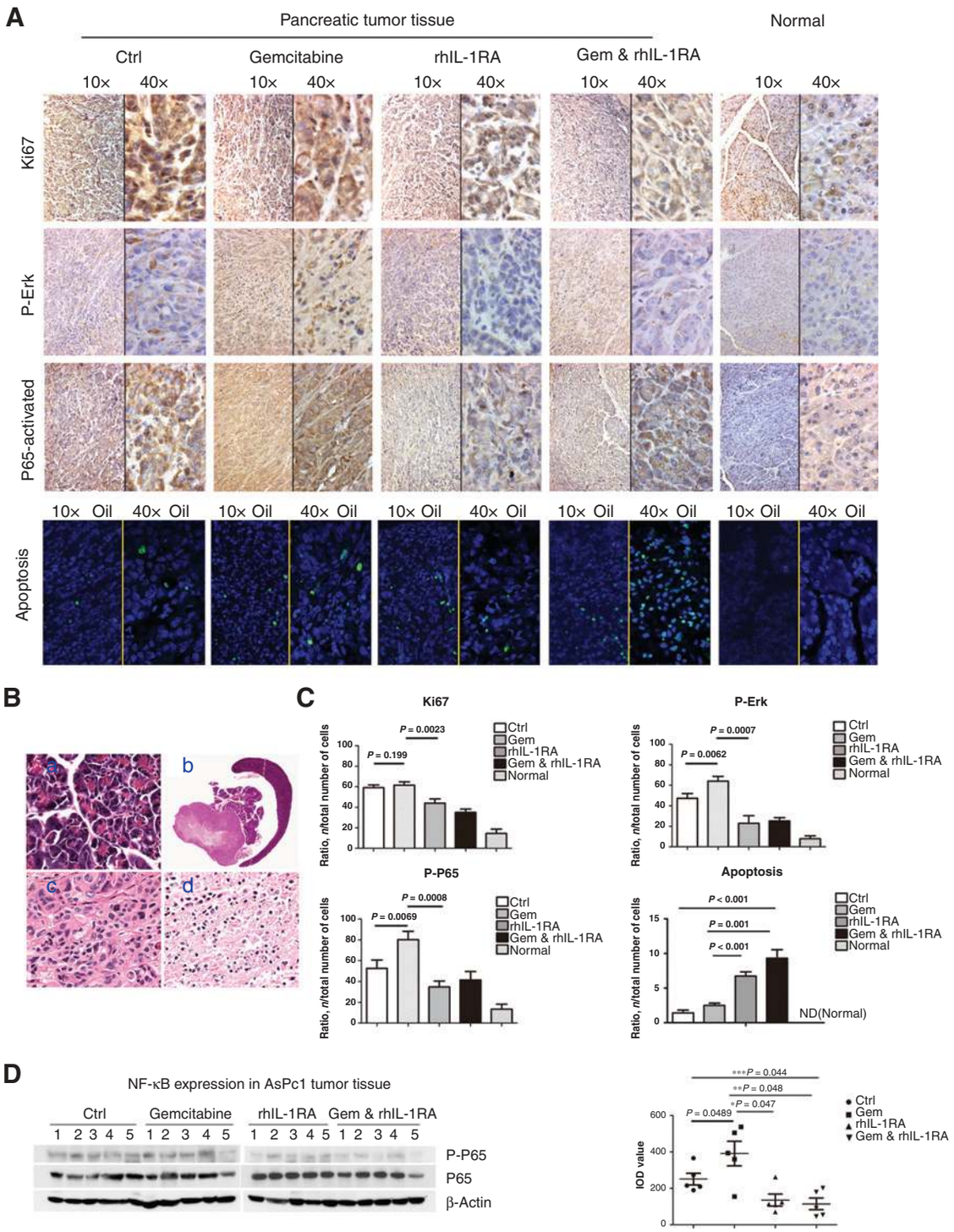

Figure 5.

Expression of cell proliferation–associated genes and inactivation of the NF-κB–regulated IL1α feed-forward loop. A, immunohistochemical analysis of serial paraffin-embedded sections from AsPc1 tumors and normal pancreatic tissues, treated as indicated, were stained with antibodies to Ki67, ERK phosphorylation, and the active P65 subunit of NF-κB. A TUNEL apoptosis analysis was performed by staining AsPc1 tumors and normal pancreatic tissues. B, representative micrographs show the histopathologic features by H&E staining. C, the error bars showed that Ki67, phosphorylated Erk, and phosphorylated P65 expressions in the group treated with gemcitabine and rhIL-1RA were significantly downregulated compared with that in the control and gemcitabine groups. The error bar shows more apoptotic cells in AsPc1 tumor tissue treated with gemcitabine and rhIL-1RA, as detected by the TUNEL assay, than in the control and gemcitabine groups ($P < 0.001$; $P = 0.001$). D, Western blot analysis showed the expression of phosphorylated P65 and P65 in a total cell lysate of AsPc1 tumor tissue in each mouse (left). Error bars showed that phosphorylated P65 expression in the group treated with gemcitabine and rhIL-1RA was significantly downregulated compared with that in the control and gemcitabine groups ($P = 0.044$; $P = 0.048$, right).

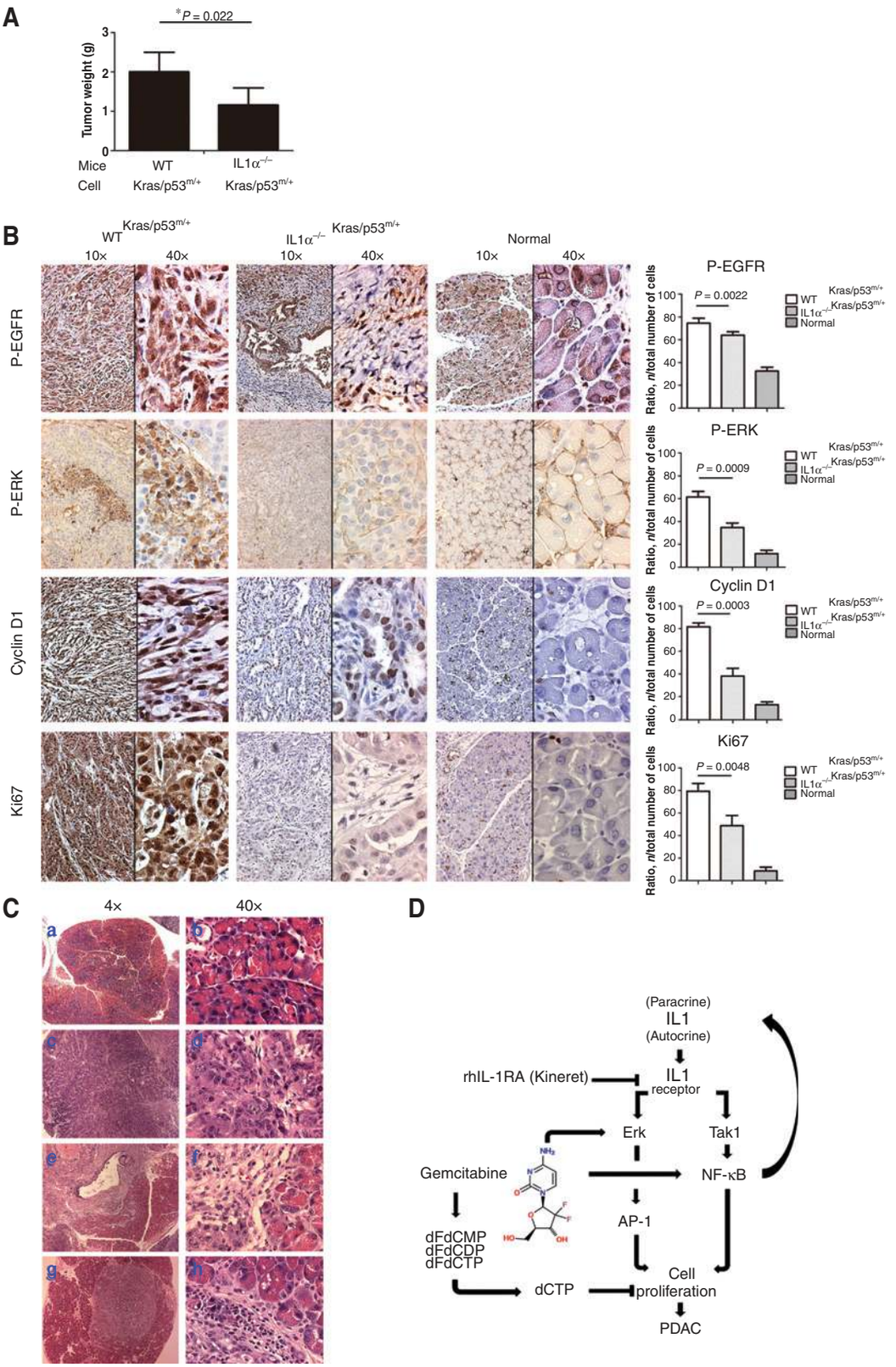

but gemcitabine-induced activation of ERK was not reduced in AsPc1 PDAC cells after treatment with rhIL1R antagonist. The Colo357, MiaPaCa-2, and HPNE/KRAS^{G12V}/p16sh cell lines were treated with rhIL-1R antagonist (10 μg/mL) for 4 hours to confirm suppression of phosphorylated NF-κB (Supplementary Fig. S1D–S1F). These results suggest that the inhibition of IL-1R by rhIL-1RA not only reduced IL-1α autocrine stimulation-induced NF-κB activation but also decreased gemcitabine-induced NF-κB activation.

Inhibition of the NF-κB–regulated IL-1α feed-forward loop increased chemosensitization of PDAC cells *in vitro*

To determine whether inhibition of NF-κB activation can sensitize gemcitabine-induced cell death, we examined the apoptotic response of PDAC cells treated with gemcitabine in the presence and absence of rhIL-1R antagonist. AsPc1 cells were treated with rhIL-1R antagonist (10 μg/mL daily), and the viable cells, as measured by the MTT assay, were significantly decreased compared with that in the control group (Fig. 3A, left). In colony-forming assay, the number of colonies that formed in AsPc1 cells also decreased with increasing doses of rhIL-1R antagonist over the 15-day treatment (Fig. 3B, left). However, a one-time treatment of rhIL-1R antagonist resulted in no change compared with the negative and positive control groups, according to the MTT and colony-formation assays (Supplementary Fig. S3A and S3B). Thus, daily treatment with rhIL-1R antagonist can enhance gemcitabine therapeutic effect (Fig. 3A, right).

The combination of gemcitabine and rhIL-1R antagonist also had a significant effect on colony formation in AsPc1 cells: there was a significant decrease in the number of colonies in the combination group (treated daily with rhIL-1R antagonist and treated once with gemcitabine) than in the gemcitabine group (Fig. 3B, right). We used flow cytometry analysis to detect apoptosis after adjuvant chemotherapy with gemcitabine and rhIL-1R antagonist. A single treatment of rhIL-1R antagonist resulted in no change in AsPc1, MiaPaCa-2, or Colo 357 cell lines (Fig. 3C). Adjuvant chemotherapy with gemcitabine and rhIL-1R antagonist was more effective in MiaPaca2 and Colo357 cells: Miacapa2 (ration of Q2: rhIL-1RA, 1.667 ± 0.120, % vs. Ctrl, 1.900 ± 0.361, %, $P = 0.5725$; gemcitabine, 6.333 ± 0.504, % vs. Ctrl, 1.900 ± 0.361, %, $P = 0.0020$; and rhIL-1RA and gemcitabine, 11.200 ± 1.002, % vs. gemcitabine, 6.333 ± 0.504, %, $P = 0.0123$; Fig. 3C); Colo357 (ration of Q2: rhIL-1RA, 4.533 ± 0.2963, % vs. Ctrl, 2.200 ± 0.231, %, $P = 0.0034$; gemcitabine, 6.100 ± 1.153, % vs. Ctrl, 2.200 ± 0.231, %, $P = 0.0295$; rhIL-1RA and gemcitabine, 12.870 ± 2.130, % vs. gemcitabine, 6.100 ± 1.153, %, $P = 0.0123$; Fig. 3C), but not in AsPc1 cells: AsPc1 (ration of Q2: rhIL-1RA, 1.733 ± 0.088, % vs. Ctrl, 1.600 ± 0.289, %, $P = 0.6815$; gemcitabine, 6.533 ± 0.933, % vs. Ctrl, 1.600 ± 0.289, %, $P = 0.0072$; and rhIL-1RA and gemcitabine, 7.667 ± 0.555, % vs. gemcitabine, 6.533 ± 0.933, %, $P = 0.3555$; Fig. 3C). The apoptotic trend was more significant in AsPc1 tumor cells that had been treated with increasing doses of rhIL-1R antagonist and gemcitabine than it was in the control group (Supplementary Fig. S3C).

To verify whether apoptosis was induced by gemcitabine in AsPc1 cells, expression levels of cleaved caspase-3, a component of the apoptotic pathway, were determined. The results show that cleaved caspase-3 was induced by gemcitabine in AsPc1 cells (Supplementary Fig. S3D, left). When we downregulated the activity of the NF-κB using 10 μg/mL rhIL-1RA combined with 10 μmol/L of gemcitabine, the expression levels of cleaved caspase-3 were increased in the AsPc1 cell line (Supplementary Fig. S3D, right). To determine whether the combination treatment reduces cell invasion and migration *in vitro*, we conducted Matrigel invasion and wound-healing assays. A Matrigel invasion chamber test showed that increasing doses of rhIL-1R antagonist could inhibit AsPc1 cell invasion (Fig. 3D, top), and increasing doses of rhIL-1R antagonist combined with 10 μmol/L of gemcitabine resulted in more inhibition of AsPc1 cell invasion (Fig. 3D, bottom). The wound-healing test showed that AsPc1 cells had increasing difficulty merging after increasing doses of rhIL-1R antagonist; they were, ultimately, unable to merge completely (Supplementary Fig. S3E). These results suggest that rhIL-1R antagonist–mediated inhibition of NF-κB activation suppressed invasion of PDAC cells.

Treatment of PDAC with anakinra alone or in combination with gemcitabine inhibited tumorigenesis in an orthotopic xenograft tumor model

To demonstrate whether inhibition of NF-κB activation by blocking the NF-κB–regulated IL-1α feed-forward loop increased the efficacy of chemotherapeutic agents in inhibiting PDAC cell growth in an orthotopic xenograft nude mouse model, 20 mice were orthotopically injected with AsPc1 human PDAC cells and randomly assigned to four groups ($n = 5$ per group). Tumors in the control group were treated with PBS (100 μL/mouse) for 4 weeks and were significantly larger than those in the experimental groups. The orthotopic xenograft PDAC tumor was found in pancreatic tissue (Supplementary Fig. S4A, yellow arrow), and the metastatic tumor in the liver tissue was close to pancreatic tissue (Supplementary Fig. S4A, black arrow). There were no metastases on the gastric or splenic tissues (Supplementary Fig. S4A, blue arrow, red arrow). The orthotopic xenograft tumor showed an absence of normal pancreatic cell morphologic features on histologic analysis (Fig. 5B, b, c and d). However, the mice treated with the combination of rhIL-1R antagonist and gemcitabine demonstrated a statistically significant reduction in tumor size compared with the control group (Fig. 4B and C). The mice treated with only gemcitabine had smaller tumors than did the control group, but there was no significant difference with rhIL-1R antagonist group (Fig. 4B and C). Thus, adjuvant

Figure 6.

A, KRAS/p53$^{m/+}$ tumors were divided from the pancreatic tissue of genetically engineered mice ($n = 5$ per group) that had been euthanized by carbon dioxide inhalation after being injected with tumor cells after 3 weeks (left). The tumor weights tested in each group showed that tumor growth was delayed in IL-1α$^{-/-}$ mice compared with WT mice ($P = 0.022$, right). B, immunohistochemical analysis of serial paraffin-embedded sections from KRAS/p53$^{m/+}$ tumors and normal pancreatic tissues that had been stained with antibodies to EGFR phosphorylation, ERK phosphorylation, cyclin D1, and Ki67. C, H&E staining observed under micrographs showed the histopathologic features of normal pancreatic tissue, tumor tissue, and the tumor margin. D, microenvironmental IL-1α is required for tumor growth. Treatment with rhIL-1RA and gemcitabine decreased tumor growth by downregulating the NF-κB–regulated IL1α feed-forward loop and the ERK pathway in PDAC.

chemotherapy with gemcitabine and rhIL-1R antagonist significantly inhibited tumor growth compared with that in the control group (Fig. 4B and C). Nude mice tumor weight (g): Ctrl group: 1.12 g, 1.84 g, 1.22 g, 0.87 g, 0.57 g; gemcitabine group: 0.98 g, 1.03 g, 0.68 g, 0.59 g, 0.3 g; rhILRA group: 1.08 g, 1.14 g, 0.69 g, 0.60 g, 1.02 g; gemcitabine and rhILRA group: 0.53 g, 0.48 g, 0.54 g, 0.32 g, 0.38 g.

Immunohistochemical analyses were carried out to determine the expressions of Ki67, ERK, and NF-κB. The P65-activated subunit of NF-κB was downregulated after IL-1α-activated NF-κB was blocked by rhIL-1R antagonist. The ERK pathway was also downregulated by rhIL-1R antagonist (Fig. 5A and C). A Western blot analysis showed that the expression of phosphorylated P65 in AsPc1 tumor tissue treated with gemcitabine was significantly higher than that in the control group (Fig. 5D). The expression level of phosphorylated P65 in AsPc1 tumor tissue treated with rhIL-1R antagonist and gemcitabine was significantly reduced compared with the control and gemcitabine groups (Fig. 5D). Thus, tumor growth was reduced with low expression of Ki67; a TUNEL assay revealed that apoptosis was increased (Fig. 5A). Taken together, these results show that adjuvant chemotherapy with gemcitabine and rhIL-1R antagonist significantly inhibited PDAC development in mouse model.

IL-1α in PDAC microenvironment is required for PDAC development in a genetically engineered mouse model

A genetically engineered mouse model was utilized to determine the role of IL-1α in the microenvironment and the dependence of PDAC on IL-1α from the host and the tumor. IL-1α$^{-/-}$ mice ($n = 5$), which were orthotopically injected with KRAS/p53$^{m/+}$ tumor cells, had significantly lower tumor weights than did WT mice after 3 weeks (Supplementary Fig. S5A). KRAS/P53$^{m/+}$ cell line was established from PDAC found in pancreas of Pdx1-cre/KRAS$^{LSL\text{-}G12D}$/p53$^{LSL\text{-}R273H}$ mice, and it is tumorigenic as shown in Fig. 6A. After KRAS/p53$^{m/+}$ mouse tumor cells (10×10^5 cells/mouse) were injected into the pancreatic tissue of WT mice, the tumors grew more rapidly in comparison with those grown in IL-1α$^{-/-}$ mice (Fig. 6A). In the absence of IL-1α in the pancreas of the host, orthotopic xenograft KRAS/p53$^{m/+}$ mouse tumors showed decreased expression of phosphorylated EGFR, phosphorylated ERK, cyclin D1, and Ki67, as determined via immunohistochemical analyses (Fig. 6B). A pathologic analysis showed presence of typical morphologic features of orthotopic PDAC (Fig. 6C). PDAC metastases were observed in liver tissues (Supplementary Fig. S5B). In this preliminary experiment, paracrine IL-1α had more effect on tumor growth than did autocrine IL-1α; therefore, systematic adjuvant treatment with IL-1α receptor inhibitor should be the preferred treatment for blocking the NFκB and IL-1α activities, thereby downregulating the activated subunit of NF-κB (Fig. 6D). Our study revealed a potential approach to inhibit NF-κB activation by targeting IL-1R, as it serves as a mechanistic link to mutant KRAS and may be clinically useful for treating PDAC.

Discussion

Recent studies showed that knocking out of IKK2/β, the kinase required for NF-κB activation, suppressed PDAC development (6, 27, 28). We further demonstrated the mechanism through which KRAS^{G12D} induced constitutive NF-κB activation (6). Briefly, constitutive activation of NF-κB is dependent on KRAS^{G12D}/AP-1–induced IL1α overexpression, which, in turn, activates NF-κB and its target genes IL-1α and p62 to initiate IL-1α/p62 feed-forward loops for inducing and sustaining NF-κB activity (6). This further enhances IL-1α/p62 expression, leading to inflammation and tumorigenesis. Thus, our findings suggest NF-κB is a missing mechanistic link between mutant KRAS, inflammation, and PDAC. Our findings also suggest IL-1α is a potential therapeutic target for PDAC patients.

To inhibit mutant RAS proteins directly with small-molecule inhibitors has been tried for more than 30 years (7). Thus far, it has proved unsuccessful. The new ideas are to find key signaling pathways that function downstream of RAS, and inhibiting such signaling pathways may lead to PDAC suppression. To test this approach, we identified that IL1α overexpression is an important mechanistic link between mutant KRAS and NF-κB activation and correlated with poor survival in PDAC patients (6, 29). IL-1β also affects the invasive potential of malignant cells and carcinogenesis. Because IL-1α is targeted by therapeutic FDA-approved IL-1R antagonist as drugs for other diseases, such as chronic inflammation autoimmune disorders, pharmacologically targeting IL1α overexpression by blocking IL-1R may improve PDAC patient survival.

To further define the role of IL-1α overexpression in PDAC development, we first knocked out IL-1α in Pdx1-KRAS$^{LSL\text{-}G12D}$; p53$^{M/+}$ mice and found that tumorigenesis is reduced in comparison with the control mice expressing IL-1α. The results suggest that overexpression of IL-1α plays an important role in PDAC development. To further determine the dependence of PDAC development on IL-1α from the host tumor environment, we injected IL-1α-null and WT mice with KRAS/p53$^{m/+}$ tumor cells. IL-1α-null mice with the PDAC cells had significantly lower tumor weights than WT mice after 3 weeks (Supplementary Fig. S4A). After KRAS/p53$^{m/+}$ mouse tumor cells were injected into the pancreatic tissue of WT mice, the tumors grew more rapidly in comparison with those grown in IL-1α$^{-/-}$ mice (Fig. 6A). These results revealed that PDAC-induced IL-1α expression from the cells of the microenvironment promotes PDAC development. Taken together, these results suggest that pharmacologically targeting IL-1α overexpression by blocking IL-1R may inhibit PDAC development. The rationales for determining the role of stromal/host derived IL-1α in activation of NF-κB and other pathways are as follows: in the tumor microenvironment, IL-1 has local effects on host infiltrating lymphocyte, endothelial, and stromal cells via a paracrine mechanism that results in production of proangiogenic and prometastatic mediators. IL-1 stimulated tumor cells through autocrine and paracrine mechanisms, which, in turn, activate other signaling pathways, such as NF-κB. IL-1 receptor also functions as a mechanistic link between mutant KRAS and NF-κB pathway required for mutant KRAS-induced PDAC. Thus, IL-1 receptor is an important therapeutic target in a number of diseases and pathologic conditions, including pancreatic cancer, rheumatoid arthritis, atherosclerosis, diabetes mellitus type I, inflammatory bowel disease, and other autoimmune disorders (30, 31).

To determine a potential pharmacologic approach to target IL-1α overexpression, we tested an inhibitor for IL-1 receptor, a human IL-1R antagonist (Anakinra). rhIL-1R antagonist is a potent receptor inhibitor, resulting in inhibition of NF-κB activity. Cell proliferation, migration, and invasion of PDAC cells treated with rhIL-1R antagonist and rhIL-1R antagonist with gemcitabine

were reduced compared with the control cells. We found that anakinra, an FDA-approved drug for certain autoimmune diseases, inhibits IL-1 receptor, and when given with or without gemcitabine, can reduce tumor growth by inhibiting IL-1α-induced NF-κB activity; this result suggests that it is a potential useful therapeutic approach for PDAC.

In conclusion, Anakinra (rhIL-1R antagonist) is an FDA-approved drug that inhibits IL1R and can be used to downregulate the activation of the NF-κB; combined with gemcitabine, rhIL-1R antagonist can significantly reduce tumor growth.

Disclosure of Potential Conflicts of Interest

No potential conflicts of interest were disclosed.

Authors' Contributions

Conception and design: Z. Zhuang, J. Ling, P.J. Chiao
Development of methodology: Z. Zhuang, H. Ju, X. Fan, J. Ling, M. Wu
Acquisition of data (provided animals, acquired and managed patients, provided facilities, etc.): Z. Zhuang, H. Ju, T. Gocho, H. Li, H. Lee, Z. Li, J.B. Fleming
Analysis and interpretation of data (e.g., statistical analysis, biostatistics, computational analysis): Z. Zhuang, H. Ju, H. Li, H. Zhou, J. Ling, M. Li, P.J. Chiao
Writing, review, and/or revision of the manuscript: Z. Zhuang, M. Aguilar, H. Lee, J. Ling, M. Li, D. Melisi, J.B. Fleming, P.J. Chiao
Administrative, technical, or material support (i.e., reporting or organizing data, constructing databases): Z. Zhuang, H. Li, X. Fan, J. Ling, Z. Li, J. Fu, J.B. Flemings
Study supervision: Z. Zhuang, T. Iida

Acknowledgments

The authors thank Dr. Hung's laboratory for providing technical imagining equipment, Ann M. Sutton in scientific publications department of MD Anderson for editorial assistance, and Yu Cao for technical support.

Grant Support

This research was supported in part by grants from the NCI (CA 097109 and CA 109405, to P.J. Chiao), from Viraph Foundation (to P.J. Chiao), and a Cancer Center Support grant to MD Anderson (CA16672).

The costs of publication of this article were defrayed in part by the payment of page charges. This article must therefore be hereby marked *advertisement* in accordance with 18 U.S.C. Section 1734 solely to indicate this fact.

Received December 30, 2014; revised August 19, 2015; accepted September 6, 2015; published OnlineFirst October 23, 2015.

References

1. Kidiyoor A, Schettini J, Besmer D, Rego S, Nath S, Curry J, et al. Pancreatic cancer cells isolated from Muc1-null tumors favor the generation of a mature less suppressive MDSC population. Immunology 2014;5:1–14.
2. Hruban H, Goggins M, Parsons J, Kern E. Progression model for pancreatic cancer. Clin Cancer Res 2000;6:2969–72.
3. Haoqiang Y, Alec CK, Costa AL, Sujun H, Gerald CC, Eliot FS, et al. Oncogenic KRAS maintains pancreatic tumors through regulation of anabolic glucose metabolism. Cell 2012;149:656–70.
4. Meredith AC, Filip B, Yaqing Z, Jean-Christophe B, Stefanie G, Craig JG, et al. Oncogenic KRAS is required for both the initiation and maintenance of pancreatic cancer in mice. J Clin Invest 2012;122:639–53.
5. Dajee M, Lazarov M, Zhang JY, Cai T, Green CL, Russell AJ, et al. NF-kappaB blockade and oncogenic RAs trigger invasive human epidermal. Nature 2003;421:639–43.
6. Ling J, Kang Y, Zhao R, Xia Q, Lee D, Chang Z, et al. KRASG12D-induced IKK2/β/NF-κB activation by IL-1α and p62 feedforward loops is required for development of pancreatic ductal adenocarcinoma. Cancer Cell 2012;21:105–20.
7. Bryant KL, Mancias JD, Kimmelman AC, Der CJ. KRAS: feeding pancreatic cancer proliferation. Trends Biochem Sci 2014;39:91–100.
8. MGysin S, Salt M, Young A, McCormick F. Therapeutic strategies for targeting ras proteins. Genes Cancer 2011;2:359–72.
9. Melisi D, Chiao P. NF-κB as a target for cancer therapy. Expert Opin Ther Targets 2007;11:133–44.
10. Niu J, Li Z, Peng B, Chiao PJ. Identification of an autoregulatory feedback pathway involving interleukin-1α in induction of constitutive NF-κB activation in pancreatic cancer cells. J Biol Chem 2004;279:16452–62.
11. Niu J, Li Z, Peng B, Chiao PJ. Identification of an autoregulatory feedback pathway involving interleukin-1α in induction of constitutive NF-κB activation in pancreatic cancer cells. J Biol Chem 2004;279:16452–62.
12. Wang Z, Li Y, Ahmad A, Banerjee S, Azmi AS, Kong D, et al. Pancreatic cancer. Understanding and overcoming chemoresistance. Nat Rev Gastroenterol Hepatol 2011;8:27–33.
13. Brown M, Cohen J, Arun P, Chen Z, Van Waes C. NF-κB in carcinoma therapy and prevention. Expert Opin Ther Targets 2008;12:1109–22.
14. May M, D'Acquisto F, Madge L, Glöckner J, Pober J, Ghosh S. Selective inhibition of NF-κB activation by a peptide that blocks the interaction of NEMO with the IκB Kinase complex. Science 2000;289:1550–4.
15. Melisi D, Xia Q, Paradiso G, Ling J, Moccia T, Carbone C, et al. Modulation of pancreatic cancer chemoresistance by inhibition of TAK 1. J Natl Cancer Inst 2011;103:1190–204.
16. Delphine L, Magali P, Davy H, Sonia DS, Cedric B, Florence C, et al. Kineret/IL-1ra blocks the IL-1/IL-8 inflammatory cascade during recombinant panto valentine leukocidin triggered pneumonia but not during *S.aureus* infection. PLos One 2014;9:e97546.
17. Rajasekaran S, Kruse K, Kovey K, Davis AT, Hassan NE, Ndika AN, et al. Therapeutic role of anakinra, an interleukin-1 receptor antagonist, in the management of secondary hemophagocytic lymphohistiocytosis/sepsis/multiple organ dysfunction/macrophage activating syndrome in critically ill children. Pediatr Crit Care Med 2014;15:401–8.
18. Lee KM, Nquyen C, Ulrich AB, Pour PM, Ouellette MM. Immortalization with telomerase of the Nestin-positive cells of the human pancreas. Biochem Biophys Res Commun 2003;301:1038–44.
19. Chang Z, Ju H, Ling J, Zhuang Z, Li Z, Wang H, et al., Cooperativity of oncogenic K-ras and downregulated p16/INK4A in human pancreatic tumorigenesis. PLoS One 2014;9:e101452.
20. Arend WP, Malyak M, Guthridge CJ, Gabay C. Interleukin-1 receptor antagonist role in biology. Annu Rev Immunol 1984;16:27–55.
21. Freireich EJ, Gehan EA, Rall DP, Schmidt LH, Skipper HE. Quantitative comparison of toxicity of anticancer agents in mouse, rat, hamster, dog, monkey, and man. Cancer Chemother Rep 1966;50:219–44.
22. Andrews NC, Faller DV. A rapid micropreparation technique for extraction of DNA-binding proteins from limiting numbers of mammalian cells. Nucleic Acids Res 1991;19:2499.
23. Burnette WN. "Western blotting": electrophoretic transfer of proteins from sodium dodecyl sulfate—polyacrylamide gels to unmodified nitrocellulose and radiographic detection with antibody and radioiodinated protein A. Anal Biochem 1981;112:195–203.
24. Towbin H, Staehelin T, Gordon J. Electrophoretic transfer of proteins from polyacrylamide gels to nitrocellylose sheets: procedure and some applications. Proc Natl Acad Sci U S A 1979;76:4350–4.
25. Weixin W, James LA, Douglas BE, Lillie L, Karen RC, Paul JC. The nuclear factor-κB RelA transcription factor is constitutively activated in human pancreatic adenocarcinoma cells. Clin Cancer Res 1999;5:119–27.
26. Arora S, Bhardwaj A, Singh S, Srivastava S, McClellan S, Nitodi C, et al. An undesired effect of chemotherapy: gemcitabine promotes pancreatic cancer cell invasiveness trough reactive oxygen species-dependent, nuclear factor

κB-and hypoxia-inducible factor 1α-mediated up-regulation of CXCR4. J Biol Chem 2013;288:21197–207.
27. Haojie H, Yan L, Jaroslaw D, Sebastian G, Jun C, Huamin W, et al. Activation of nuclear factor-κB in acinar cells increases the severity of pancreatitis in mice. Gastroenterology 2013;144:202–10.
28. Eleni M, Maud B, Natalie C, Juliana BC, Nia ES, Sergei AN, et al. Crosstalk between the canonical NF-κB and Notch signaling pathways inhibits Pparγ expression and promotes pancreatic cancer progression in mice. J Clin Invest 2011;121:4685–99.
29. Melisi D, Niu J, Chang Z, Xia Q, Peng B, Ishiyama S, et al. Secreted interleukin-1alpha induces a metastatic phenotype in pancreatic cancer by sustaining a constitutive activation of nuclear factor-kappaB. Mol Cancer Res 2009;7:624–33.
30. Lewis AM, Varghese S, Xu H, Alexander HR. Interleukin-1 and cancer progression: the emerging role of interleukin-1 receptor antagonist as a novel therapeutic agent in cancer treatment. J Transl Med 2006;4:48.
31. Dinarello CA. Why not treat human cancer with interleukin-1 blockade? Cancer Metastasis Rec 2010;29:317–29.